Lattice-Dynamical Aspects of the Antiferroelectric Phase Transition in $ND_4D_2PO_4$†

H. MEISTER
Euratom, Ispra, Italy and Brookhaven National Laboratory, Upton, New York 11973
AND
J. SKALYO, JR., B. C. FRAZER, AND G. SHIRANE
Brookhaven National Laboratory, Upton, New York 11973
(Received 7 March 1969)

Temperature-dependent quasi-elastic neutron scattering has been observed in the paraelectric tetragonal phase of $ND_4D_2PO_4$ in the vicinity of the Z point of the Brillouin zone, i.e., at $(h,0,l)$ where $h+l$ is odd. The data are interpreted in terms of a condensing highly damped optic-phonon mode which initiates the transition to the antiferroelectric state. The intensity contours of the quasi-elastic scattering in the (a^*,c^*) plane are roughly elliptical in shape and are centered at the Z points of the extended Brillouin zone. The major axis of the intensity distribution is parallel to the c^* direction and is about four times larger than the a^*-oriented minor axis, thus suggesting a polarization fluctuation perpendicular to c^*. As the temperature is lowered, the integrated intensities at the Z points increase as $T/(T-T_0)$. The value for T_0 of 195°K compares more closely with the actual transition temperature ($T_n=234$°K) than that obtained by dielectric constant measurements ($T_0\approx80$°K). The inelasticity of the scattering is 0.7 ± 0.1 meV at 244°K and increases linearly with temperature to 1.8 ± 0.2 meV at 304°K. An interpretation of the scattering at the Z point in terms of an overdamped phonon mode results in a damping constant independent of temperature and a temperature dependence of the frequency of the form $\omega_A^2\propto K(T-T_0)$. In the antiferroelectric phase, the Z points become permissible Bragg peaks and quasi-elastic scattering is not observed.

I. INTRODUCTION

THE paraelectric phase of the hydrogen-bonded antiferroelectric $NH_4H_2PO_4$ (abbreviated ADP) is isomorphous with that of the well-known ferroelectric prototype KH_2PO_4 (abbreviated KDP). In both compounds a large isotope shift of the transition temperature occurs on substitution of deuterium for hydrogen, thus demonstrating the important role of the hydrogen bonds in the transition mechanism.

The paraelectric structure of ADP has been established by x-ray and neutron-diffraction measurements.[1–4] The space group is $I\bar{4}2d$ with four molecules in the body-centered tetragonal unit cell. The space group of the antiferroelectric phase, as determined by x rays,[3] is $P2_12_12_1$, and with the now primitive unit cell there is no body-centered condition on permissible Bragg reflections. The transition results in only a slight orthorhombic distortion of the original cell; hence, there are still four molecules per cell. This is in contrast to KDP, which transforms to $Fdd2$ symmetry with eight molecules in an enlarged orthorhombic cell, and no additional Bragg peaks are permitted.[5] The redefinition of the unit cell from body-centered to face-centered in this case is accompanied by doubling of the cell size with crystallographic axes in the ab plane rotated by 45°. One may note that the c/a ratios for KDP and for ADP are such that the Brillouin zones differ in appearance.

By far the most important structural feature of both KDP and ADP in their two phases is the $(H_2PO_4)^{-1}$ network in which each phosphate group is linked by O—H···O hydrogen bonds to a tetrahedral arrangement of phosphate group neighbors. A significant difference between the two structures, however, is that in ADP each ammonium group is tetrahedrally connected to four phosphate groups by N—H···O hydrogen bonds. While the Slater[6] model for ordering of the O—H···O hydrogen bonds in KDP has been verified by neutron diffraction,[7] the ordering in ADP is assumed to follow the description given by Nagamiya[8] and independently by Mason and Matthias.[9] The hydrogen ordering schemes for KDP and ADP are given in Fig. 1.

An interpretation of ferroelectric transitions on the basis of lattice dynamics has been given by Anderson[10] and by Cochran.[11] Cochran has shown that in ionic crystals long-range Coulomb forces, arising dynamically from polarization fluctuations, can cancel the short-range interatomic forces and lead to a lattice instability at the transition temperature. As the temperature is decreased toward the transition, this effect is evidenced in the decreasing energy of a transverse-optic mode at

† Work performed under the auspices of the U. S. Atomic Energy Commission.
[1] R. Ueda, J. Phys. Soc. Japan 3, 328 (1948).
[2] B. C. Frazer, Ph.D. thesis, Alabama Polytechnic Institute, Auburn, Ala., 1949 (unpublished).
[3] R. O. Keeling and R. Pepinsky, Z. Krist. **106**, 236 (1955).
[4] L. Tenzer, B. C. Frazer, and R. Pepinsky, Acta Cryst. **11**, 505 (1958).
[5] B. C. Frazer and R. Pepinsky, Acta Cryst. **6**, 273 (1953).
[6] J. C. Slater, J. Chem. Phys. **9**, 16 (1941).
[7] G. E. Bacon and R. S. Pease, Proc. Roy. Soc. (London) **A230**, 359 (1955).
[8] T. Nagamiya, Progr. Theoret. Phys. (Kyoto) **7**, 275 (1952).
[9] W. P. Mason and B. T. Matthias, Phys. Rev. **88**, 477 (1952).
[10] P. W. Anderson, in *Proceedings of the Conference on the Physics of Dielectrics* (Academy of Science, U.S.S.R., Moscow, 1958), p. 290.
[11] W. Cochran, Advan. Phys. **9**, 387 (1960); **10**, 401 (1961).

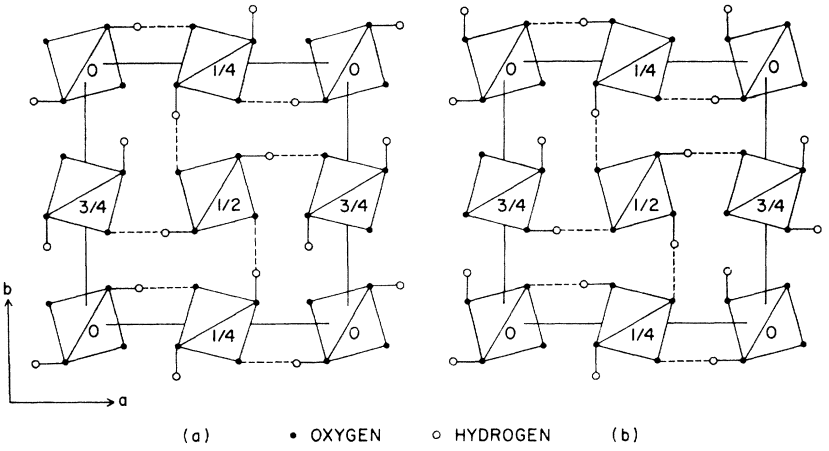

FIG. 1. (a) Positions of the hydrogen atoms in the ferroelectric structure. The heights of the centers of the PO_4 tetrahedra are shown. Axes indicated are as given by Tenzer *et al.* (Ref. 4). (b) Positions of the hydrogen atoms in the antiferroelectric structure of ADP.

the Γ point ($\mathbf{q}=0$).[12] The frequency of this mode can be related to the static dielectric constant ϵ_0 by the Lyddane-Sachs-Teller[13] relation for solids with more than two atoms per primitive cell,[14]

$$\frac{\epsilon_0}{\epsilon_\infty}=\prod_i \frac{\omega_{iLO}^2}{\omega_{iTO}^2}, \tag{1}$$

where ω_{iLO} and ω_{iTO} are longitudinal- and transverse-optical phonon frequencies, respectively, and ϵ_∞ is the high-frequency dielectric constant. If only the ferroelectric mode (ω_{1TO}) is varying with temperature, the temperature dependence of its frequency can be related to that of ϵ_0 as follows:

$$\omega_{1TO}^2=K(T-T_0). \tag{2}$$

The ferroelectric mode has been observed in KDP by Kaminow and Damen,[15] utilizing Raman scattering. The measurements indicate that the mode is highly overdamped with a damping constant independent of temperature. Deuterated KDP has been investigated with neutrons by Buyers *et al.*,[16] and the quasi-elastic scattering in the vicinity of the Γ point is reported to be consistent with the overdamped temperature-dependent ferroelectric mode. The intensity contour of the scattering as a function of $\mathbf{q}$ indicated the polarization fluctuation to be in the ferroelectric c direction.

Cochran has also argued that the antiferroelectric transition is due to a zone-boundary temperature-dependent mode which becomes unstable before the ferroelectric mode. He infers that the antiferroelectric mode should occur at the Z point [$\mathbf{q}=(2\pi/c)\hat{c}$] in ADP. If the mode energy is much less than the ferroelectric mode energy, the temperature dependence of ϵ_0 as given by Eq. (1) will not be anomalous. A slowly varying temperature dependence for ϵ_0 was, in fact, measured for ADP by Busch,[17] and similar behavior has been observed in deuterated ADP.[9] The present paper reports observation of critical scattering of neutrons at the Z points in $ND_4D_2PO_4$, and the results are interpreted as a manifestation of a highly overdamped antiferroelectric mode ω_A.

II. EXPERIMENTS

A. Sample Description and Experimental Apparatus

Two deuterated ADP single crystals ($2\times2\times2$ cm^3) were used in the present measurements. These were supplied by the Isomet Corporation with a specified $(99.2\pm0.2)\%$ degree of deuteration. In the course of the neutron experiments, the transition temperature T_N was measured to be (234.0 ± 0.3)°K for both samples. In passing through the transition to the antiferroelectric phase, an ADP crystal shatters into a mass of well-oriented adhering fragments. Consequently, the transition can be readily detected with neutrons through the sharp increase in Bragg peak intensities due to the great reduction in extinction effects. Dielectric constant measurements of Mason and Matthias[9] on a sample inferred to be $\approx100\%$ deuterated gave a transition temperature of 242°K, and recent work by Vasilevskays *et al.*[18] reports a value of 240°K for a crystal of $(96\pm1)\%$ deuteration. These results would imply a deuteration level of only $\approx91\%$ in the present samples.

Both crystals were mounted in sample containers in a He atmosphere to prevent deuterium loss during

[12] Notation after G. F. Koster, in *Solid State Physics*, edited by F. Seitz and D. Turnbull (Academic Press Inc., New York, 1957), Vol. 5, p. 201.
[13] R. H. Lyddane, R. G. Sachs, and E. Teller, Phys. Rev. **59**, 673 (1941).
[14] W. Cochran, Z. Krist. **112**, 465 (1959).
[15] I. P. Kaminow and T. C. Damen, Phys. Rev. Letters **20**, 1105 (1968).
[16] W. J. L. Buyers, R. A. Cowley, G. L. Paul, and W. Cochran, in *Neutron Inelastic Scattering* (International Atomic Energy Agency, Vienna, 1968), Vol. 1, p. 267.
[17] G. Busch, Helv. Phys. Acta **11**, 269 (1938).
[18] A. S. Vasilevskaya, E. N. Volkova, V. A. Koptsik, L. N. Rashkovich, T. A. Regul'skaya, I. S. Rez, A. S. Sonin, and V. S. Suvorov, Kristallografiya **12**, 518 (1967) [English transl.: Soviet Phys.—Cryst. **12**, 446 (1967)].

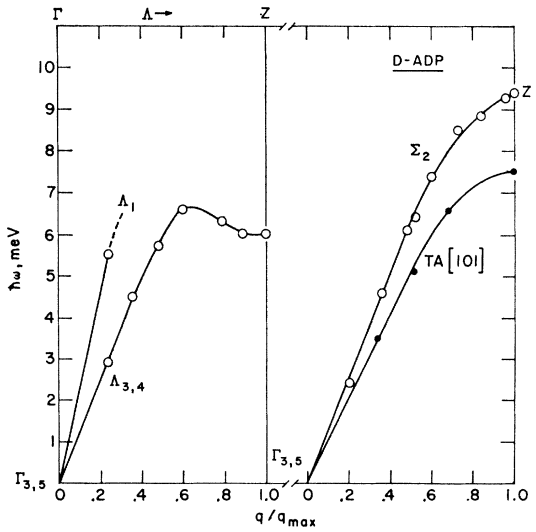

FIG. 2. Lower branches of dispersion curves at 244°K. Measurements were made on an (010) zone. Symmetry points are after Koster (Ref. 12), while the subscripted representations are after Kovalev (Ref. 20); TA[101] is not a symmetry mode and is labeled descriptively. Λ_3 and Λ_4 are degenerate.

storage and to promote thermal equilibrium during measurements. The crystals were mounted with their b axes vertical to permit measurements in the a^*c^* plane. The sample container was fastened thermally and mechanically to the temperature-controlled copper block of a cryostat. Regulation and measurement of temperature was made to an accuracy of ± 0.1°K, employing a platinum resistance thermometer.

Neutron scattering measurements were carried out on a triple-axis spectrometer at the Brookhaven High-Flux Beam Reactor. The (311) and (111) planes of germanium were used in the monochromator and analyzer positions ($\frac{1}{2}\lambda$ contamination is thereby eliminated). The incident neutron energy varied between 26 and 65 meV, depending on the nature of the measurement. The particular germanium reflection, neutron energy, and beam collimation employed varied in accordance with the desired spectrometer energy resolution.[19] Relatively poor energy resolution can be used to advantage to effectively integrate the energy-broadened quasi-elastic scattering. On the other hand, high-resolution conditions are necessary in making measurements near Bragg reflections, in order to avoid interference from low-energy acoustic modes and to give increased detail to intensity contours near the Z points.

TABLE I. Quasi-elastic intensities I at $(h,0,l)$ with $h+l$ odd.

(h,k,l)	I	(h,k,l)	I	(h,k,l)	I
1,0,2	185±25	1,0,6	60±20	7,0,4	60±20
2,0,1	40±20	6,0,1	<40	1,0,8	<100
2,0,3	60±20	4,0,5	<40	8,0,1	270±30
3,0,2	110±20	5,0,4	270±30	3,0,8	50±20
1,0,4	120±20	3,0,6	<20	8,0,3	70±20
4,0,1	110±20	6,0,3	<20	2,0,9	110±20
3,0,4	50±20	2,0,7	230±30	9,0,2	220±30
4,0,3	60±20	7,0,2	165±25	4,0,9	70±20
2,0,5	40±20	5,0,6	175±25	9,0,4	120±20
5,0,2	50±20	4,0,7	90±20		

[19] M. J. Cooper and R. Nathans, Acta Cryst. 23, 357 (1967).

B. Antiferroelectric Mode

An initial search was made at 244°K for well-defined soft phonons near the zone boundary. Figure 2 shows the lowest-energy acoustic branches of the dispersion curves measured by the constant-$\mathbf{Q}$ technique with a fixed final energy of 40 meV. Measurements were made from the (800), (008), and (404) Bragg points. A well-defined soft phonon was not observed, but an extensive search for an overdamped phonon mode revealed the antiferroelectric mode at the Z points of the Brillouin zone, $(h,0,l)$ with $h+l$ odd.

In order to sample a relatively large region in reciprocal space, the incoming neutron energy was chosen at 50 meV; and with the resulting large probe, the energy-broadened peak was effectively integrated in the intensity measurement. A list of the 29 observations made in the a^*c^* plane is given in Table I.

The scattering cross section for an overdamped normal mode is given by

$$\frac{d^2\sigma}{d\Omega d\omega} \propto |F(\mathbf{Q})|^2 \frac{kT}{\omega_A^2} \frac{\omega_A^2/\Gamma}{\omega^2+(\omega_A^2/\Gamma)^2}. \tag{3}$$

Here $|F(\mathbf{Q})|$ is the inelastic structure factor, ω_A is the undamped mode frequency, and Γ is the damping constant. The relation has been written for the case where

$$\Gamma/2\omega_A \gg 1,$$

and results in a quasi-elastic energy broadening of $2\hbar\omega_A^2/\Gamma$.

If one assumes by analogy to the ferroelectric case that the antiferroelectric mode frequency is related to the temperature by

$$\omega_A^2 = K(T-T_0), \tag{4}$$

then the mode frequency in the vicinity of the Z points can be approximated by

$$\omega_A^2(\mathbf{q},T) \propto [(T-T_0)+f(\mathbf{q}_Z-\mathbf{q})]. \tag{5}$$

Introducing the relations

$$\gamma = 2\omega_A^2/\Gamma \quad \text{and} \quad \Delta\mathbf{q} = \mathbf{q}_Z - \mathbf{q},$$

Eq. (3) can be expressed as

$$\frac{d^2\sigma}{d\Omega d\omega} \propto |F(\mathbf{Q})|^2 \frac{kT}{(T-T_0)+f(\Delta\mathbf{q})} \frac{\frac{1}{2}\gamma}{\omega^2+(\frac{1}{2}\gamma)^2}. \tag{6}$$

While a detailed analysis leading to a uniquely determined dynamical model cannot be made for ADP

with the limited intensity data in Table I, the observed quasi-elastic scattering will be examined in terms of Eq. (6). Emphasis will be placed on the intensity contours, the energy broadening, and the temperature dependence of the integrated intensity at the Z points.

C. Intensity Distribution

A detailed mapping of the quasi-elastic intensity contours about the Z point (5,0,4) was made at 244°K with an energy resolution of 0.68 meV FWHM (full width at half-maximum). As shown in Fig. 3, the contours are elliptical with the semimajor axis along c^* about four times larger than the semiminor axis along a^*.

With an energy resolution of 1.65 meV FWHM, scans were made through the (5,0,4) point in the a^* and in the c^* directions giving the same elliptical extension as above. The scan in the a^* direction is shown in Fig. 4. These cross scans were made at various temperatures between 244 and 304°K. Over this range, the relative changes in FWHM were within the limits of measurement error (<20%) and indicated that the $\Delta\mathbf{q}$ FWHM is essentially independent of temperature. The experimental points of each scan could be fitted

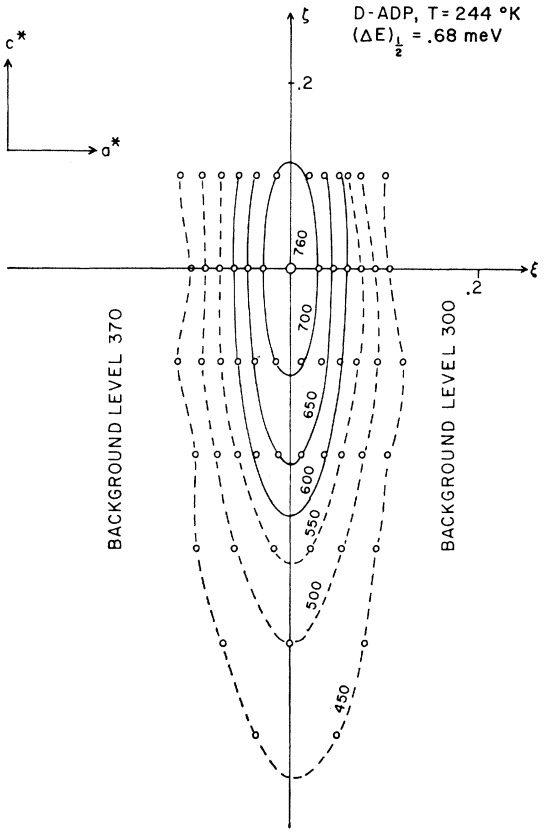

FIG. 3. Intensity contour around (5,0,4). Spectrometer set for elastic scattering.

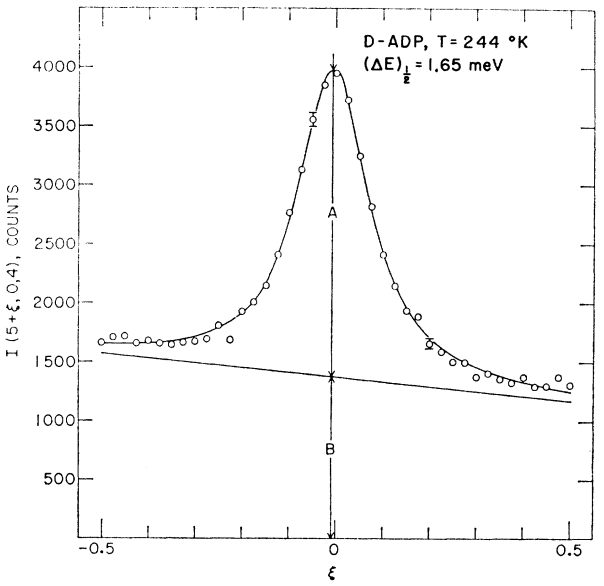

FIG. 4. $\bar{Q}$ scan in a^* direction across (5,0,4) for elastic scattering at 244°K. Solid lines: least-squares fit to experimental data with a Lorentzian plus a linear background.

quite satisfactorily by a Lorentzian superimposed on a linear background, as shown in Fig. 4.

Similar cross scans were also made for (1,0,2), (2,0,7), and (5,0,6). The results at all points were much the same for (5,0,4). This suggests that the inelastic structure factors $|F(\mathbf{Q})|^2$ in Eq. (6) are varying very slowly in the vicnity of the Z point. With this assumption, the above scans give information about $f(\Delta\mathbf{q})$, which represents the dispersion of the undamped mode near the Z point.

Since the distribution has a $\Delta\mathbf{q}$ FWHM independent of temperature, the temperature dependence of $f(\Delta\mathbf{q})$ should be very nearly

$$f(\Delta\mathbf{q})=(T-T_0)g(\Delta\mathbf{q}), \tag{7}$$

where $g(\Delta\mathbf{q})$ is independent of temperature. This means that the curvature of the ω_A dispersion curve at the Z point decreases as the transition temperature is approached. In addition, the predominant term in $g(\Delta\mathbf{q})$ would be quadratic in order to explain the good fit of the intensity profiles by Lorentzians, i.e.,

$$f(\Delta\mathbf{q})=(T-T_0)(\Delta\mathbf{q}\cdot\mathbf{A}\cdot\Delta\mathbf{q}+\cdots). \tag{8}$$

Finally, the shape of the contour is such that

$$A_{xx}\approx 16A_{zz} \quad \text{and} \quad A_{xz}=0.$$

This is an important characteristic of the antiferroelectric mode, since it indicates that the polarization fluctuations are strong within the ab plane. This is in contrast to critical scattering due to the ferroelectric mode in deuterated KDP, for which polarization fluctuations are parallel to the c axis.[16]

D. Temperature Dependence

Integration of Eq. (6) over frequency indicates that the observed integrated intensity at the Z point should vary as $T/(T-T_0)$. An instrumental resolution of 1.65 meV FWHM was used in obtaining line profiles by the constant-Q method at (5,0,4). Background corrections were made by subtracting averages of two line profiles made on either side of the Z point in a region of negligible quasi-elastic scattering. The line profiles were numerically integrated from -2.6 to $+2.6$ meV, and the inverse of the integrated intensity is plotted as a function of $(T-T_0)/T$ in Fig. 5. The figure is drawn for a value of $T_0=195$°K. The deviation of the highest-temperature point may possibly be due to some systematic neglect of the wings of the Lorentzian line profiles. The crosses in Fig. 5 indicate data taken on a double-axis spectrometer with a neutron energy of 65 meV. This method of energy integration, while giving a high background, agrees very well with the triple-axis data.

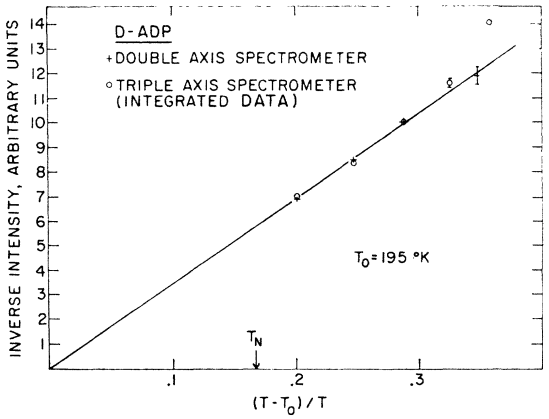

FIG. 5. Inverse quasi-elastic intensity at (5,0,4) as function of reduced temperature $(T-T_0)/T$, with $T_0=195$°K.

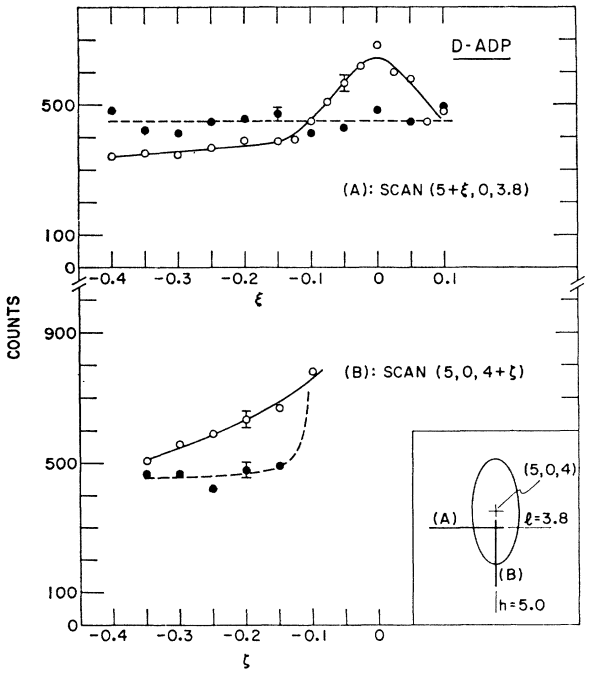

FIG. 6. Two different scans A and B (see their traces in inserted picture, in which ellipse symbolizes quasi-elastic intensity distribution in paraelectric phase) taken as sample temperatures of (○) 244 and (●) 230°K, respectively.

The departure of T_0 from the measured transition temperature of 234°K is not unexpected, as the antiferroelectric transition of ADP is of first order. The present value of T_0 is quite close to the transition temperature, however, in comparison with the value ($T_0\simeq 80$°K) obtained by dielectric constant measurements.[9]

In the low-temperature phase, the quasi-elastic scattering disappears and is replaced by a Bragg peak. This can be seen in Fig. 6 for the case of scans made in the vicinity of (5,0,4) at 244 and 230°K.

E. Inelasticity

The inelasticity of the antiferroelectric mode at the Z point is given by Eq. (3) as $2\hbar\omega_A^2/\Gamma$ FWHM. Since ω_A^2 depends linearly on $T-T_0$, as shown above, the dependence of the inelasticity on temperature would reveal the temperature dependence of Γ.

The constant-Q method was utilized to measure line profiles at the Z point. Background corrections were made as described previously. The instrument resolution was calibrated by measuring the incoherent elastic scattering profile of a vanadium sample. A typical measurement at (5,0,4) at 244°K is shown in Fig. 7.

Least-squares analysis of the profiles gave a value of (0.69±0.02) meV FWHM for a Gaussian fit to the

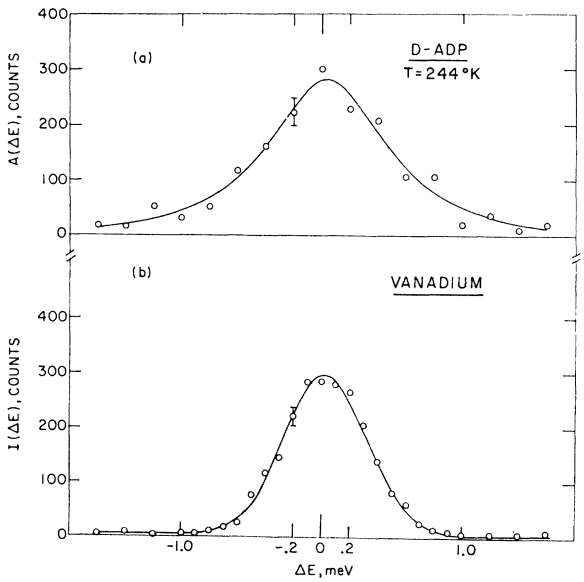

FIG. 7. (a) Energy scan of quasi-elastic signal $A(\Delta E)$ at (5,0,4), background subtracted, sample temperature 244°K. Solid line: Fitted Lorentzian gives FWHM=1.04±0.13 meV. (b) Energy scan $I(\Delta E)$ with vanadium sample, same conditions as with (a). Solid line: Fitted Gaussian gives FWHM=0.695±0.015 meV.

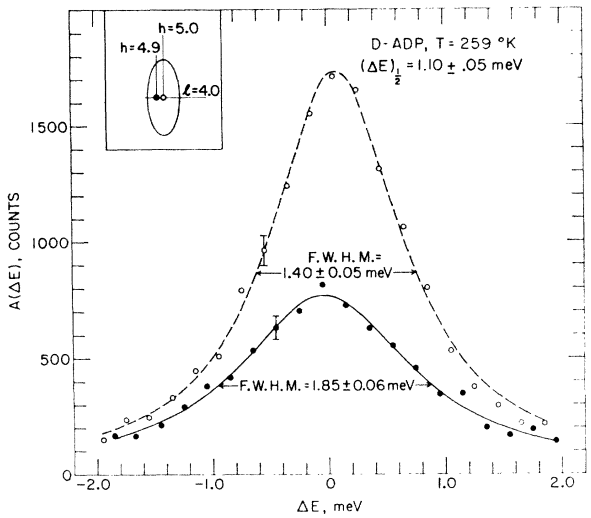

FIG. 8. Energy scans of quasi-elastic signal $A(\Delta E)$ at (5,0,4) and (4.9,0,4), background subtracted, sample temperature 259°K. Lines: fitted Lorentzians.

vanadium calibration. A Lorentzian fit to the ADP quasi-elastic scattering gave a FWHM of 1.04±0.13 meV. The inelasticity was then obtained by the square root of the difference of the squares. While strictly valid only for Gaussians (within the accuracy of the measurements), the approximation involved is a reasonable one. Similar measurements made at (1,0,2) and (2,0,7) were in good agreement with the (5,0,4) data, and the three cases gave an average of 0.7±0.1 meV FWHM for quasi-elastic broadening at 244°K.

Figure 8 illustrates two line profiles measured at 259°K with an instrumental resolution of 1.10±0.05 meV FWHM. The line profile through the Z point has a FWHM of 1.40±0.05 meV resulting from an inelasticity of 0.9±0.15 meV. Figure 8 also displays a line profile taken at (4.9,0,4) which indicates increased inelasticity for $\Delta\mathbf{q}\neq 0$.

The inelasticity at (5,0,4) is plotted as a function of temperature in Fig. 9. A linear extrapolation of the data gives a value of $T=210$°K for $\omega_A^2/\Gamma=0$. This is in reasonable agreement with the value of 195°K obtained in Sec. II D. Within the accuracy of the present measurements, therefore, Γ would appear to be independent of temperature. This observation is similar to the Kaminow-Damen[15] results on KH_2PO_4, where Γ is independent of temperature for the ferroelectric mode.

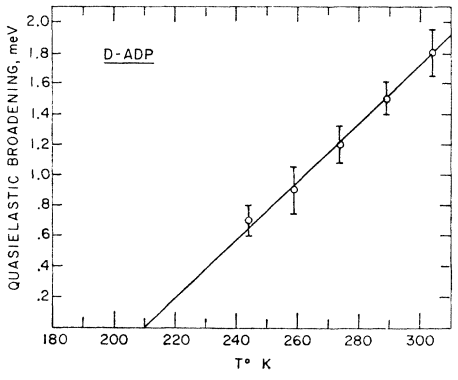

FIG. 9. Quasi-elastic broadening as function of sample temperature.

III. CONCLUDING REMARKS

Quasi-elastic neutron scattering has been observed at the Z point of the Brillouin zone in the paraelectric phase of deuterated ADP. The scattering was investigated as a function of temperature, energy, and $\mathbf{q}$. The results are consistent with a lattice-dynamical interpretation of the antiferroelectric transition.

A determination of the atomic movements in the antiferroelectric mode could greatly facilitate model calculations pertinent to the properties of ADP. In principle, this mode could be identified in deuterated ADP by comparing calculated inelastic structure factors, $|F(\mathbf{Q}, \mathbf{q}=(2\pi/c)\hat{\epsilon})|^2$, with the observed quasi-elastic intensities listed in Table I. A unique solution of this rather complex problem is hardly possible with the present data, however. The problem involves determination of 20 amplitude parameters corresponding to a linear combination of the 20 modes, Z_1+Z_4.[20] These two types of irreducible representations are degenerate by time reversal so that all amplitudes can be chosen as real. A further complication is that the Debye-Waller parameters are probably not known with sufficient accuracy to be considered fixed, and would have to be treated as additional variables.[3,4]

In this situation, only a few of the most obvious and simplest model possibilities were examined. The results were not very promising. While these proceeded basically from an assumption of hydrogen movements in the O—H···O bond system according to the Nagamiya scheme,[8] the lack of success in the calculations does not demonstrate that this pattern of movements is incorrect. It merely indicates the importance of considering possible distortional movements of the $(PO_4)^{-3}$ and $(ND_4)^{+1}$ groups.

Clearly, more extended measurements in reciprocal space will be required before a serious attempt can be made to determine the antiferroelectric mode in ADP. Valuable insight into an analysis of the problem should be provided after the much simpler case of the ferroelectric mode in KDP has been completely determined.

ACKNOWLEDGMENT

We would like to thank John D. Axe for many helpful and stimulating comments during the course of this work.

[20] Subscripts refer to representations as given by O. V. Kovalev, *Irreducible Representations of the Space Groups* (Gordon and Breach, Science Publishers, Inc., New York, 1965).